Postprint of: Castro-Muñoz R., Msahel A., Galiano F., Serocki M., Ryl J., Hamouda S. B., Hafiane A., Boczkaj G., Figoli A., Towards azeotropic MeOH-MTBE separation using pervaporation chitosan-based deep eutectic solvent membranes, SEPARATION AND PURIFICATION TECHNOLOGY, Vol. 281 (2022), 119979, DOI: 10.1016/j.seppur.2021.119979

Towards azeotropic MeOH-MTBE separation using pervaporation chitosan-based deep eutectic solvent membranes

Roberto Castro-Muñoz[1,2*], Asma Msahel[3,4], Francesco Galiano[5*], Marcin Serocki[6], Jacek Ryl[7], Sofiane Ben Hamouda[3,8], Amor Hafiane[3], Grzegorz Boczkaj[1*], Alberto Figoli[5]

[1]Gdansk University of Technology, Faculty of Chemistry, Department of Process Engineering and Chemical Technology, 11/12 Narutowicza St., 80-233, Gdansk, Poland

[2] Tecnologico de Monterrey, Campus Toluca. Av. Eduardo Monroy Cárdenas 2000 San Antonio Buenavista, 50110, Toluca de Lerdo, Mexico.

[3] Laboratory of Water Membrane and Environmental Biotechnology (LMBE), CERTE BP 273, 8020 Soliman, Tunisia

[4] Department of Chemistry, University of Tunis El-Manar, Farhat Hached University Campus, BP n° 94 Rommana, 1068 Tunis, Tunisia

[5]Institute on Membrane Technology, ITM-CNR, Via P. Bucci 17/c, 87036 Arcavacata di Rende (CS), Italy

[6]Department of Pharmaceutical Technology and Biochemistry, Faculty of Chemistry, Gdansk University of Technology, 11/12 Narutowicza St., 80-233, Gdansk, Poland

[7] Department of Electrochemistry, Corrosion and Materials Engineering, Faculty of Chemistry, Gdansk University of Technology, 11/12 Narutowicza St., 80-233, Gdansk, Poland

[8] NANOMISENE Laboratory, LR16CRMN01, Centre for Research on Microelectronics and Nanotechnology (CRMN) of Technopole of Sousse B. P334, 4054 Sahloul Sousse, Tunisia

*E-mail: food.biotechnology88@gmail.com ; castromr@tec.mx (R. Castro-Munoz)

grzegorz.boczkaj@pg.edu.pl (Grzegorz Boczkaj) ; f.galiano@itm.cnr.it (F. Galiano)

---

*Corresponding Author

Abstract

Deep eutectic solvents (DESs) are a new class of solvents that can offset some of the major drawbacks of common solvents and ionic liquids. When dealing with the preparation of dense membranes, the use of DESs is still challenging due to their low compatibility with the polymer phase. In this research, a novel L-proline:sulfolane (molar ratio 1:2) DES was synthesized and used for the preparation of more sustainable bio-based membranes using chitosan (CS) as a polymer phase. The compatibility among both phases (polymer and DESs) and their ability to form homogenous membranes was preliminary studied. In this regard, scanning electron and confocal microscopies were used to completely map the structure of the resulting membranes evidencing a complete homogenous structure. The membranes were also characterized in terms of contact angle (CA), Fourier transformed infrared spectroscopy (FTIR), mechanical resistance and swelling degree (uptake). Preliminary pervaporation tests for the separation of a methanol (MeOH)- methyl *tert*-butyl ether (MTBE) azeotropic mixture were, thus, performed. In this regard, the addition of DESs provided an enhanced separation efficiency in comparison to pristine CS membranes. Thanks to the morphology and properties exhibited, the newly developed membranes can be considered as excellent bio-based candidates to be explored in other gas selective and solvent oriented membrane operations.

Keywords: Deep eutectic solvents; membrane preparation; chitosan; methanol/MTBE; pervaporation.

1. Introduction

According to the "*Twelve Principles of Green Chemistry*" established by Anastas and Warner [1], there is a big need of implementing green materials and processes in the manufacturing of new products. Therefore, the research community is continuously exploring the potentialities of new feedstocks to follow such principles aiming at the preservation of the environment [2]. Today, deep eutectic solvents (DESs), which are a new class of solvents, have been categorized as "green alternatives" to conventional solvents for various applications, including metal plating and coatings [3], sustainable media in organic reactions [4], extraction and separation of biologically active compounds from natural sources [5], CO_2 capture [6], desulfurization [7], as stationary phases for chromatography [8], enzymatic biodiesel production [9], chemical and biocatalysis [10], to mention just a few. DESs overcome most of the major drawbacks of common solvents and ionic liquids, together with several advantages, such as low toxicity, low cost, easy handling, biodegradability, biocompatibility and reusability [11]. Typically, DESs are synthesized by combining hydrogen bond acceptor (HBA), like quaternary ammonium salt, with hydrogen bond donor (HBD) compounds [3].

When dealing with membrane preparation, DESs have been primarily proposed and used as additives in the manufacture of DES-liquid supported membranes [12,13], with the aim of enhancing the separation properties of polymeric membranes. The superior

performance exhibited by DESs based membranes are generally attributed to a facilitated molecule transport and adsorption through the functional groups of DESs [14–16]. DESs have been also explored as pore forming agents in the fabrication of asymmetric membranes via phase-inversion method [17].

To the best of our knowledge, there are no studies employing DESs in the preparation of non-porous (well-known as dense) membranes. This is because, fundamentally, the compatibility of DESs and polymer phases, for their complete merging, is still a challenge. Therefore, in this work, we describe the successful incorporation of a specific DES (L-proline:sulfolane) into chitosan (CS) membranes surmounting one of the most common constraints related to the proper dispersion of the DES into the polymer matrix.

In order to achieve this goal, a hydrophilic and water-soluble DES, such as L-proline:sulfolane (molar ratio 1:2), was firstly synthesized. Afterward, its ability to form dense homogenous membranes was evaluated using CS as a continuous polymer phase. The cross-linking effect on membrane properties and performance was also evaluated using glutaraldehyde (GA). To evaluate their miscibility, the complete blending of both phases (DES and polymer) was studied by mapping the complete membrane structure. For this purpose, scanning electron microscopy (SEM) and scanning confocal electron microscopy (SCEM), were employed. Secondly, the generated membranes were also characterized in terms of contact angle (CA), Fourier transformed infrared spectroscopy (FTIR), mechanical test and swelling degree (uptake). Preliminary pervaporation tests towards the methanol (MeOH)- methyl *tert*-butyl ether (MTBE) separation have been performed in order to prove the applicability of the new synthesised membranes.

2. Methodologies

2.1. Reactants and materials

L-proline (purity ≥98 %, Sigma Aldrich), sulfolane (purity ≥99 %, Alfa Aesar), phosphoric acid (purity ≥85 %, POCH S.A.) and GA (grade II, 25 wt%) were acquired and used without further purification. CS (medium molecular weight) was acquired from Sigma Aldrich. MeOH (99.8%) and MTBE (99.7%) were also purchased from Sigma-Aldrich (St. Louis, USA) and used without further purification.

2.2. DES synthesis

L-proline:sulfolane, at a molar ratio (1:2), was synthesized. Basically, 32.4 g of L-proline (0.282 mol), 67.6 g of sulfolane (0.564mol) and 705 mL of phosphoric acid 1M (0.705 mol) were mixed at 1000 rpm (70°C) until obtaining a transparent solution. Lately, the excess of water was removed out by means of a rotary vacuum evaporator (Rotavapor R-300 with a V-300 vacuum pump, BUCHI).

2.3. Membrane preparation

CS-DES membranes were prepared via dense-film casting method and solvent evaporation. The CS dope solutions (1.5 wt.%) in acidic water solutions were prepared. Herein, an acetic acid solution (2wt.% in distilled water) was preliminarily prepared. The polymer dope solutions were stirred over 24 h (at room temperature). Later, 5 wt.% of DES (L-proline:sulfolane), with respect to CS concentration, was separately added in the respective dope solutions. The resulting mixture was stirred for 4 h before applying the *in-situ* cross-linking procedure. The latter procedure was utilized to ensure the entrapment

of the DES into the polymer phase, in which chemical cross-linking with GA was used [18]. Here, *in situ* cross-linking procedure was carried out by adding 100 µL of GA and 100 µL of HCl (to speed up the reaction) to every dope. This was stirred for 15 min, cast on clean Petri dishes and then dried at room temperature for 2 days. The final appearance of membranes was of a homogeneous and transparent film with approximately 25 µm of thickness. To sum up, the prepared membranes were labelled as follows: pristine CS, cross-linked CS (xCS), chitosan:L-proline:sulfolane (CS:PRO:SUF) and cross-linked chitosan: L-proline:sulfolane (xCS:PRO:SUF).

2.4. Membrane characterization

2.4.1. *Scanning electron microscopy (SEM).* The morphological structure of the membrane surface and cross-section was preliminarily analysed using a SEM instrument (Hitachi S-3400N, Japan), operating with a tungsten electron source. The secondary electron detector was used for the analysis, and micrographs were made under 5 kV accelerating voltage. Before the microanalysis, a 10 nm layer of metallic gold was sputtered at each sample surface to compensate the low surface conductivity. The corresponding images were acquired at suitable magnification. In the case of cross-section analysis, all samples were prepared by cryogenic fracture after immersion in liquid N_2.

2.4.2. *Scanning confocal electron microscopy (SCEM).* In order to assess the homogeneity and dense structure of the resulting membranes, a complete scanning of the structure was performed using a LSM 800 T-PMT confocal microscope (Carl Zeiss AG, Oberkochen, Germany) with a CCD camera [19]. Images were acquired and

processed with ZEN Blue software.

2.4.3. *Fourier transformed infrared spectroscopy (FTIR)*. FTIR was performed on all membrane formulations described previously using a Nicolet iS10 FTIR (Thermo Fisher Scientific) spectrometer equipped with a DTGS detector and a Golden Gate diamond ATR accessory. The spectra were recorded in the 4000–400 cm^{-1} wave number range at a resolution of 16 cm^{-1}.

2.4.4. *Water contact angle (CA)*. The water contact angle measurements were performed using ultrapure water by the method of the sessile drop using a goniometer OCA15 (Data Physics). The average and standard deviation values were determined for three measurements.

2.4.5. *Mechanical test.* Mechanical properties of pristine CS and xCS:PRO:SUF membranes were measured using a Zwick/Roell Z2.5 test unit (BTC-FR2.5TN-D09, Germany). Measurements were performed at room temperature (25 °C) using a membrane sample of 1 × 5 cm. The samples were extended at the constant elongation rate of 5 mm min^{-1} until their break. Elongation at break, Young's modulus and tensile strength were, then, determined. Each sample was analyzed at least four times, the results were expressed as the average and standard deviation. Mechanical tests were carried out on all the investigated membranes before and after use in PV tests (14.3 wt% MeOH; 85.7 wt% MTBE).

2.4.6. Uptake. The degree of swelling (uptake) of the membranes was determined for pure feed components (MeOH, MTBE), various MeOH-MTBE mixtures (5, 10 25, 50, wt.% MeOH) as well as azeotropic mixture (14.3% MeOH and 85.7% MTBE). Three small pieces of membranes (1 × 5 cm) were weighed and immersed in the solvent mixtures at

30 °C for 48 h. The wet membrane samples were quickly wiped with tissue paper to remove the excess free liquid on their surface and immediately weighed with a digital balance (Gibertini, Crystal 500, Italy, Crystal 500, Gibertini Elettronica srl, Milan, Italy) with an accuracy of 0.001 g. In general, the uptake was calculated as follows:

$$Uptake\ (\%) = \frac{W_w - W_d}{W_d} \cdot 100 \qquad \text{Eq. (1)}$$

where W_w and W_d correspond to the weight of the wet and dry membranes, respectively.

2.5. Pervaporation tests

The PV experiments were performed in a laboratory-scale setup, whose graphical drawing and details can be found elsewhere [20]. Basically, a mixture (250 mL) of an azeotropic MeOH-MTBE (14.3–85.7 wt.%, respectively) solution was poured in the pervaporation cell. The feed operating temperature was varied (at 25, 35, 45 °C) and controlled with an accuracy of 0.01 °C using a thermo digital circulating bath (Neslab RTE-201, USA). The vacuum on the permeate side (at 0.05 mbar) was maintained by using a RV5 two-stage vacuum pump (Edwards, UK).

The membrane, having an active area of 9.6 cm^2, was placed on a porous support within the membrane cell. The permeated vapour was condensed and collected in a glass trap placed in a liquid nitrogen condenser. Once reached the steady-state, the permeates were collected for 5 h of experiment and immediately weighted to determine the total permeate flux. The permeate flux (J) was determined as follows:

$$J = \frac{Q}{A \cdot t} \qquad \text{Eq. (2)}$$

where Q corresponds to the weight of the permeate (expressed in kg), A corresponds to the membrane area (m^2) and t is the operating time (h). The partial flux (J_i) for each component i was calculated by multiplying its weight fraction (y_i) in the collected permeate sample by the total permeate flux (J), as follows:

$$J = Y_i \cdot J \qquad \text{Eq. (3)}$$

The separation factor (α) was calculated according to the following equation:

$$\alpha = \frac{y_{MeOH}/y_{MTBE}}{x_{MeOH}/x_{MTBE}} \qquad \text{Eq. (4)}$$

where y and x correspond to the weight fractions of the components in the permeate and feed, respectively. The permeate composition was determined by an Abbe 60 type direct reading refractometer (Bellingham + Stanley Ltd., UK) at 25 °C. The J and α values were expressed as the average of more than two runs to ensure the accuracy of the outcomes.

3. Results and discussion

3.1. *Scanning electron microscopy (SEM).*

In general, all resulting membranes showed a smooth and uniform surface pattern without signs of plastic deformation, being common for dense polymeric membranes [21]. Particular attention has been devoted to the cross-section analyses of the membranes, as shown in **Figure 1**. For instance, the pristine CS membrane (Figure 1a) displayed a crater-like pattern, which is commonly generated during deformation caused by the freeze-fracture of polymer membranes. Such a pattern has been well documented in

pristine [22] and cross-linked CS membranes [18]. Regarding the CS blend with PRO:SUF (Figure 1c), the membrane exhibited a more homogeneous dense pattern structure with non-visible pores. Similarly, cross-linked CS-DESs membranes (Figure 1d) confirmed a dense structure with non-visible defects among the phases and additives (like DES agent). Particularly, such characteristics can be used as an evidence of the good miscibility of the hydrophilic PRO:SUF DES in CS, as demonstrated in other polymer/polyethylene glycol blends [23,24].

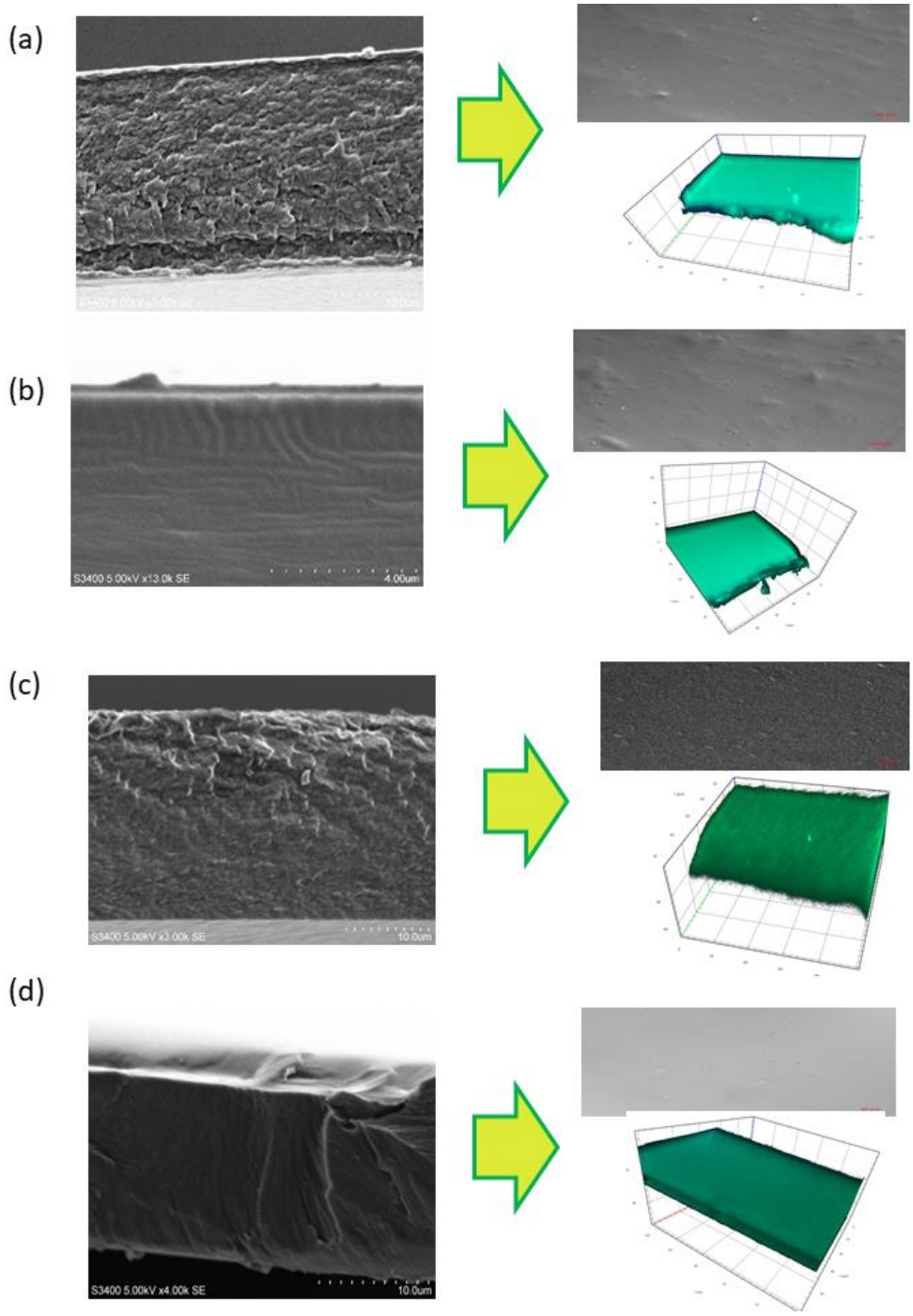

Figure 1. SEM cross-section, surface view and 3D view images of the prepared membranes based on CS and DES. (a) pristine CS (CS), (b) cross-linked chitosan (xCS) (c) chitosan:L-proline:sulfolane (CS:PRO:SUF), (d) cross-linked chitosan:L-proline:sulfolane (xCS:PRO:SUF).

In this work, the addition of the DES has evidenced to provide a tighter and smoother structure in CS membranes. However, in literature it has been reported that DESs are employed in the fabrication of porous membranes by acting as pore forming agents [17,25]. In general, the use of pore formers is aimed, in phase-inversion techniques, to generate large pores and voids in the membrane matrix [26]. The pore formers (such as polyethylene glycol and polyvinyl pyrrolidone) are generally removed by the membranes after its formation by washing them with water.

In our case, the approach was oriented to physically entrap the selected DES into the membrane thus exploiting the benefits that it may offer once preserved in the membrane structure. DESs have been successfully applied for the extraction, separation and purification of biomolecules due to their ability to form hydrogen bonds via dipole-dipole and other specific solute-solvent interactions [27,28].

The resulting CS-based membranes visually exhibited a dense structure. However, there is still a possibility that the used DESs can also be supported (or encapsulated) within the polymeric structure. Therefore, further analysis of the overall membrane structure were performed. In this case, SCEM was used for mapping the structures of the membranes, as detailed in **Figure 1** (right side). It is known that polymer blending with other phases strongly depends on its available chemical functionalities. If functional groups are not present between phases, a poor interaction and hence low miscibility will be obtained [29]. This is also fundamental for blending polymers with inorganic phases (e.g., nanoparticles), in which the nano-sized materials tend to be chemically functionalized to reach a good compatibility and contact between polymer and filler interfaces [30].

In particular, CS owns a plenty of amino and hydroxyl groups, making it an excellent

candidate for polymer blending [31]. Also, in the case of DESs, they may also offer a series of functional groups which can interact with CS giving to the final membrane specific properties. At this point, it is likely that this new DES employed (PRO:SUF), bearing different functional groups (such as amino, hydroxyl, and carbonyl), can interact with CS. For instance, **Figure 1** shows the surface view of the synthesized membranes confirming their smooth and homogenous surfaces with absence of pinholes and defects. Regarding the 3D view, the images were created by stacking together 210 fluorescence intensity scans of each membrane. Every single scan is a picture representation of a 0.25 μm cross-section of each membrane, each scan is created by merging green and blue from two fluorescence channels (DAPI and AF488, excitation: 353 and 493 nm, emission 465 and 517 nm, detection 400-580 nm). By scanning the membrane structure, the complete blending between CS and DES was confirmed, evidencing a dense-like morphology. Also, there was no evidence of DES phase separation or encapsulation in the polymer matrix.

3.2. *Water contact angle (CA) and Fourier transformed infrared spectroscopy (FTIR)*

The FTIR results (shown in Figure 2) can be the evidence of the affective blending of the DES into the CS polymer membrane matrix. All spectra exhibit a strong and broad non-symmetric band at about 3400 cm^{-1} that results from overlapping of the O-H and N-H stretching vibrations of functional groups engaged in hydrogen bonds. The spectrum of CS shows typical absorption bands at 1600 cm^{-1} (for C=O stretching in amide group),

1550 cm^{-1} (for N-H bending in no acetylated 2-aminoglucose) and 1560 cm^{-1} (for N-H bending in amide group), as reported in literature [32]. Absorption bands at 1100 cm^{-1}, corresponding to an antisymmetric stretching of the C-O-C bridge, 1050 cm^{-1} and 1000 cm^{-1}, related to skeletal vibrations implying the C-O stretching, are typical for CS. Interestingly, the blending of CS with DES provoked a slight shift on such characteristic polymer bands, giving a proof of the good interaction among the phases and thus compatibility. For the cross-linked CS-DES membranes with GA, they exhibit an increase in the absorption between 1600-1650 cm^{-1} which can be attributed to imine bonds N=C [33,34]. The stretching at 1540 cm^{-1}, 1710 cm^{-1} and 2900 cm^{-1} corresponds to free-aldehydic bonds and increased C-H stretch, respectively. Also, the presence of aliphatic amino groups diminishes as much as the peak 1100 cm^{-1} does. These shifts may be the reason of the more hydrophobic nature of the membranes compared to the pristine and CS-DES blends (non-cross linked) [18], which is in agreement with the CA data.

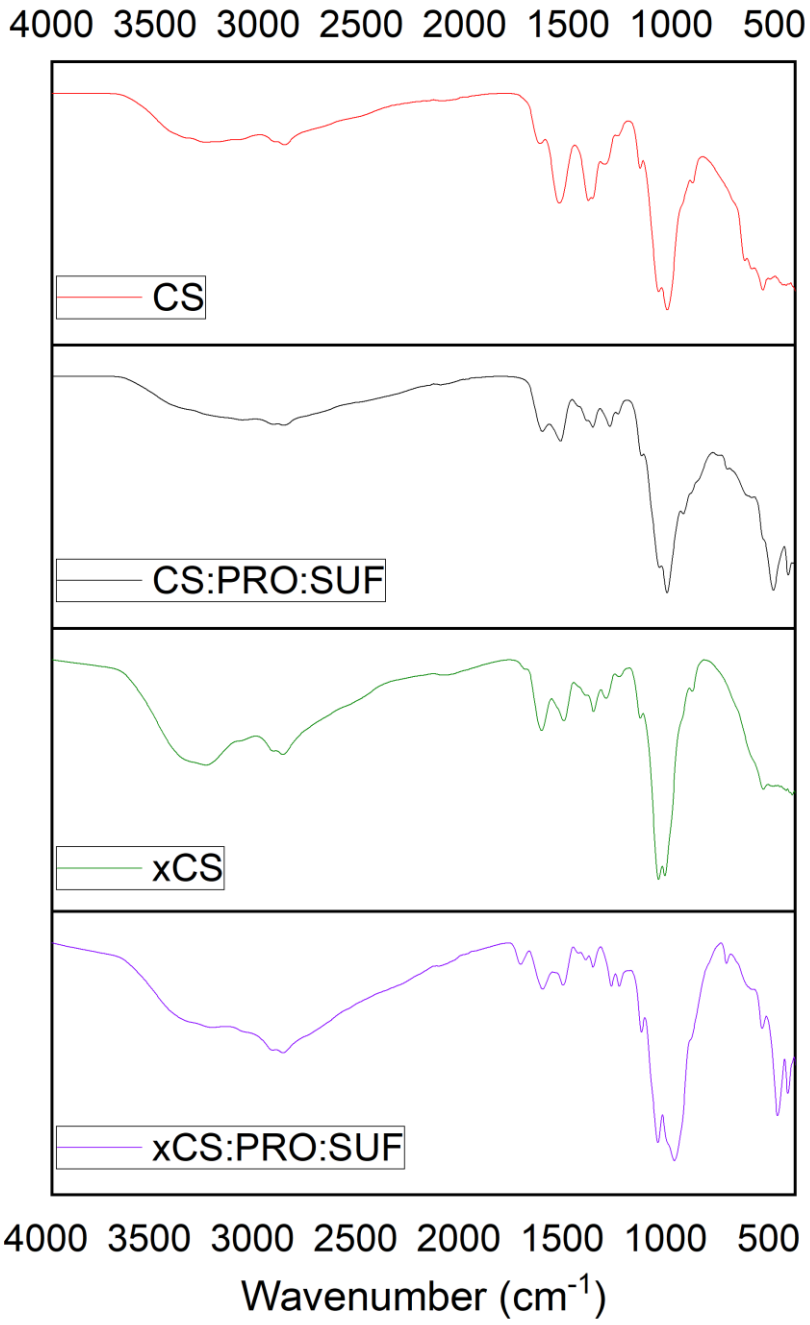

Figure 2. FTIR spectra for pristine and cross-linked CS membranes and their blends with DESs.

An important aspect to address during the incorporation of DESs in membranes deals with the possible effect on the membrane hydrophilicity/hydrophobicity. The pristine CS membrane showed a CA value of 90°, in line with the data reported in literature which place the CA of CS polymer between 84-88° [32,35]. The variability in the hydrophilic/hydrophobic nature of CS strongly depends on the deacetylation degree of the polymer; for instance, a high degree of deacetylation provides highly hydrophilic CS membranes [36], meaning more amine groups available on the CS molecule which can promote the water transport through the membrane matrix [37]. In principle, the hydrophilicity of CS belongs to its hydrophilic groups, such as -OH and $-NH_2$; however, such hydrophilicity decreases when cross-linking is applied. For this reason, the CA value reached up to 95° when CS was cross-linked.

The incorporation of the PRO:SUF DES in the CS membrane led to a drastic decrease of the contact angle value (34°). This may suggest that the polar groups provided by the DES (such as amino and carboxyl) have a big impact in enhancing the hydrophilicity of the overall membrane.

Table 1. CA values and mechanical properties of the pure CS membranes and its blends with DES.

Membrane	CA (°)	Image:	Before PV			After PV		
			Young's modulus (N/mm^2)	Tensile strenght (N/mm^2)	Elongation at break (%)	Young's Modulus (N/mm^2)	Tensile strenght (N/mm^2)	Elongation at break (%)
CS	90±0.5		415 ± 32	61 ± 9	11 ± 7	632 ± 3	65 ± 11	12 ± 4
xCS	95±0.5		1467 ± 41	40 ± 11	6 ± 2	853 ± 206	45 ± 12	9 ± 2
CS:PRO:SUF	34±2		163 ± 10	38 ± 10	16 ± 4	164 ± 19	41 ± 2	12 ± 1
xCS:PRO:SUF	89±7		226 ± 47	50 ± 13	11 ± 2	205 ± 66	35 ± 13	8 ± 1

Surprisingly, the cross-linking of the CS membrane containing DES (xCS:PRO:SUF membrane) led to an increase of the CA value (89°) close to the pristine CS membrane. It is worth mentioning that, after a cross-linking protocol, the reaction of GA with primary amino groups results in the formation of two Schiff bases involving both aldehyde groups of the GA molecule [32,38]. Herein, the decrease of the number of the $-NH_2$ groups could be the responsible of the contact angle increase in the xCS:PRO:SUF membrane.

As can be seen in **Table 1**, the blending of the DES with CS decreased specific mechanical properties, such as Young's modulus and tensile strength (with a decrease

of about 61 and 38%, respectively). However, the impact of DES addition on membrane mechanical properties was observed to be reduced when the cross-linking was adopted. In this case, the reduction of Young's modulus and tensile strength, in comparison to the pristine CS membrane, was much reduced (45 and 18%, respectively). DESs can act as plasticizers into a CS polymer matrix causing a decrease in the intermolecular interactions. The addition of plasticizers in CS, in fact, conducts to a transition from a rigid to a softer material with elastic properties [39]. In particular, the loss of tensile strength is associated to the breakup of the film network provoked by the incorporation of the additive into the polymer. Similar results have been documented in literature in CS films when mixed with different additives [40] and natural chlorine chloride/ malonic acid eutectic mixtures [41]. It has been, in fact, documented that the increase in DES concentration is responsible of the decrease of Young's modulus and tensile strength in CS [41]. On the contrary, elongation at break was surprisingly preserved by the DES addition, which has been associated with the increase in the free volume in the polymer matrix. According to Jakubowska et al. [41], a possible expansion of a free volume fosters polymeric chain translation, being worthy in the stabilization of films in the elastic flow regime. In this case, the cross-linking could have re-established the original free volume of CS films after DES blending since the elongation at break was comparable to the initial value of the CS membrane.

3.3. *Pervaporation performance*

3.3.1. Effect of operating temperature on permeation and separation factor.

The PV separation data for all tested membranes is reported in **Table 2**.

Table 2. Performance of CS-DES membranes as a function of temperature (feed composition: 14.3 wt.% MeOH; 85.7 wt.% MTBE).

Temperature	Total flux (kg m^{-2} h^{-1}) × 10^3	Separation factor (α)	MeOH partial flux (kg m^{-2} h^{-1}) × 10^3	MTBE partial flux (kg m^{-2} h^{-1}) × 10^3
	CS			
25°C	25±5	12.2± 0.11	16.9±3	8.2±2
35°C	33±2	5.6± 0.10	16.4±3	17±3
45°C	40±3	2.7± 0.09	17.4±2	27±4
	xCS			
25°C	14±2	28.8± 0.10	11±2	2±0.2
35°C	20±3	27.6± 0.10	16±3	3±0.3
45°C	29±3	24.9± 0.11	24±2	5±0.5
	CS:PRO:SUF			
25°C	44±1.5	1.3±0.21	7±0.1	33±1.7
35°C	54±0.0	1.1±0.06	8±5.7	45±0.4
45°C	73±3	1.0±0.029	11±0.8	62±2.8
	xCS:PRO:SUF			
25°C	8±2	35.4±0.15	6.8±2	1±1
35°C	8±1	31.5±0.25	7±2	1.4±1
45°C	11±3	28.5±0.22	9.2±1	2.1±1

Figure 3 graphically illustrates the effect of the feed temperature on the total permeate flux, where a permeation increase, as a function of temperature, was observed in pristine

CS membrane and its blend with DES. Such a behaviour is a typical trend in polymeric membranes since polymer chains are more flexible at higher temperatures fostering the sorption ability of the solvent molecules, conducting to an increase in permeation of compounds across the intermolecular distances of the polymeric membrane [42].

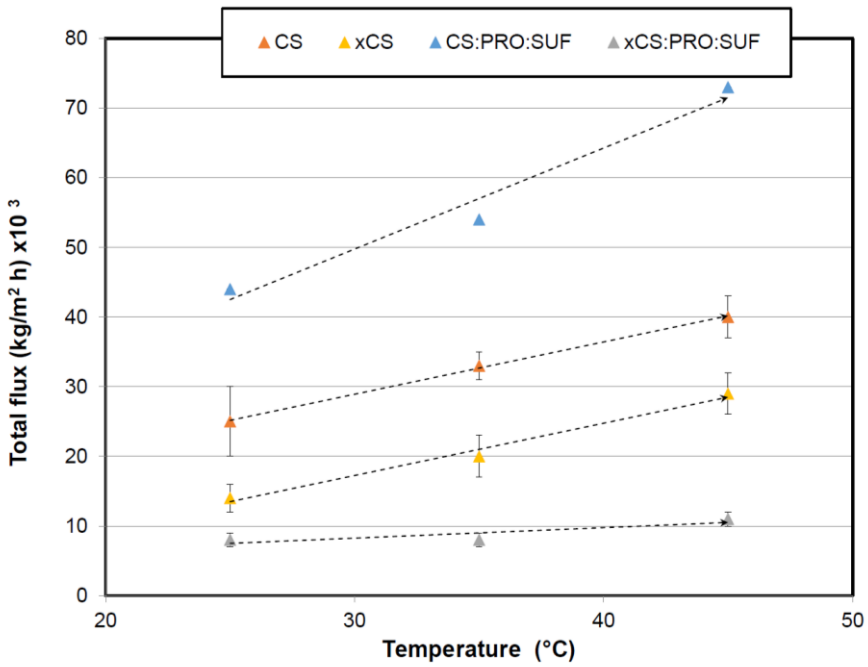

Figure 3. Effect of feed temperature on total flux (feed composition: 14.3 wt.% MeOH; 85.7 wt.% MTBE, pressure: 0.05 mbar). The curves are only guides to the eye.

The temperature dependence on permeate flux was determined by means of the Arrhenius model, as expressed in Equation 5.

$$J = J_o \cdot \exp\left(-\frac{E_A}{R \cdot T}\right) \qquad \text{Eq. (5)}$$

where J_o corresponds to the pre-exponential factor, E_a refers to the apparent

activation energy for permeation (for the mixture and each compounds) and $R \cdot T$ corresponds to the common energy term. Using the logarithms for Eq. 5. E_A can be calculated in a linear function, which confirms that an Arrhenius relationship occurs between total fluxes and operating temperature; in other words, an increase in total permeation takes places by increasing temperature. From **Table 3**, it can be seen that crosslinked CS membrane display lower E_a values for methanol (ca. 13.34 kJ/mol) than MTBE (ca. 15.66 kJ/mol), which gives an input of methanol selectivity of CS. Interestingly, the incorporation of the hydrophilic DES lowered the E_a value for methanol up to 0.49 kJ/mol in xCS:PRO:SUF membrane, while the E_a value for MTBE was less affected. At this point, the E_a decreased substantially towards MeOH compared with MTBE in the range of 25-45 °C. It is worth mentioning that the PV process in the operating temperature affects primarily the permeation rate of MeOH, and does influence minimally the MTBE transport. It is clear that the presence of DES lowers the energy needed for the molecules to permeate across the membranes and this is particularly evident for MeOH molecules. This also can be supported by the hydrophilic nature of the DES, which definitely may display a preference for polar compounds (like MeOH) [28].

Table 3. Apparent activation energies for total permeate, MeOH and MTBE partial fluxes of the CS-DES membranes.

Membrane	Activation energy values (kJ/mol)		
	Total	Methanol	MTBE
CS	8.05	5.12	20.44
xCS	12.46	13.34	15.66
CS:PRO:SUF	8.64	10.79	7.70
xCS:PRO:SUF	5.38	0.49	12.63

Regarding the selectivity, the separation factor in pristine CS membrane decreases as a function of the temperature (see **Figure 4**). Importantly, such selectivity was improved by incorporating the DES with the aid of in situ cross-linking, reaching a value up to 35 (at 25°C). In general, high separation factors and lower permeation rates were, in fact, obtained at the lowest temperatures for all membranes. This agrees with the free volume theory, which establishes that thermal motion of polymer chains in the amorphous regions induces a free volume increase. As temperature increases, the frequency and amplitude of the chain jumping (i.e., thermal agitation) increases, and consequently, the free volume becomes larger [43]. Even if the kinetic diameters of MeOH and MTBE substantially differ (3.6 and 6.2 Å, respectively), the thermal motion of the polymeric chains facilitates also the diffusion of larger molecules (like MTBE) across the membrane conducting to a decrease in the separation factor. Additionally, the separation factor decrease agrees with the fact that activation energy values for MTBE were larger than for MeOH.

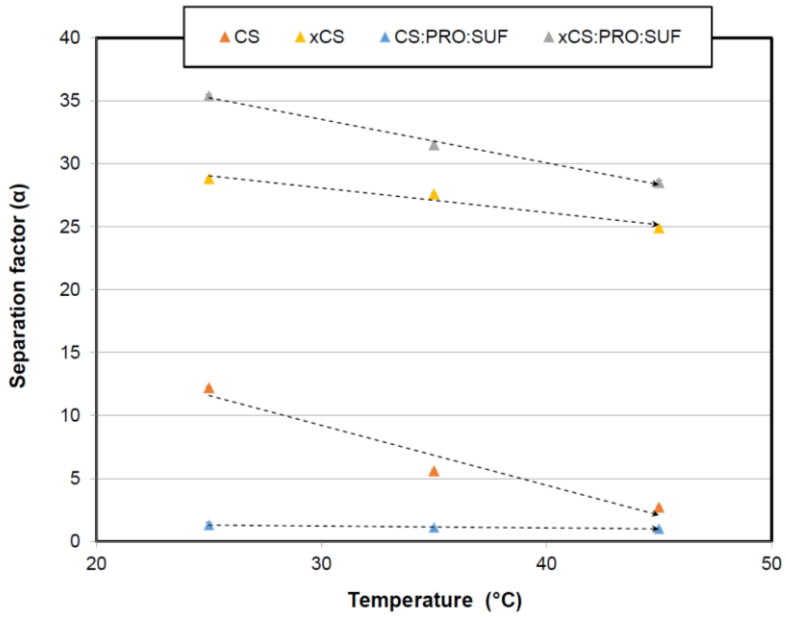

Figure 4. Effect of feed temperature on the separation factor (feed composition: 14.3 wt.% MeOH; 85.7 wt.% MTBE, pressure: 0.05 mbar). The curves are only guides to the eye.

It is important to mention that *in situ* cross-linking was required at this specific case. As can be seen in **Table 2**, the direct incorporation of DES into CS led to a loss of the selective properties of the membrane. To date, it has been documented that DES addition tends to increase the free volume in polymer matrices. According to Jakubowska et al. [41], a possible expansion of the free volumes fosters the polymeric chain translation, which, if from one side can enhance the stabilization of films at elastic flow regime (improving the elongation at break properties), from the other side it can lower the selective performance of the membrane.

Finally, the determination of the uptake properties of the studied membranes is reported in **Figure 5**. It can be seen that all membranes display low uptake values, e.g., lower

than 7%, for low MeOH concentrations (up to 10 wt.%). However, the increase of MeOH concentration in the feed mixture, led to a higher swelling of the membranes. The addition of DES caused a decrease in the solvent uptake ability of the membranes. This may support Jakubowska's hypothesis [41] that DES provides stabilization of the CS membranes. Of course, the uptake was substantially suppressed when cross-linking was applied since such a protocol makes polymer membranes more resistant to the solvent mixtures due to a higher restriction of polymer chains mobility [44]. It is well known that PV membranes which are less susceptible to swelling are preferred to guarantee more stable performance when separating organic/organic feed solutions. To point out, the membranes also exhibited, to some extent, stable mechanical properties since the properties did not change strongly after use in PV testing (see **Table 1**).

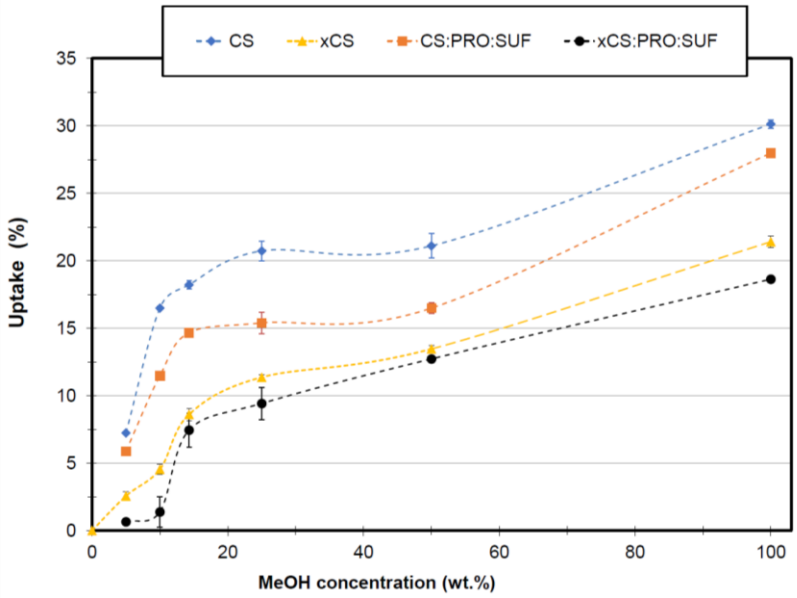

Figure 5. Uptake of CS-DES membranes at different MeOH concentrations (at 30 °C). The curves are only guides to the eye.

3.3.2. Performance comparison of CS-DES membranes with literature

As in all membrane-based technologies, it is clear that the PV performance of either polymer and composite membranes is strongly influenced by several factors, including membrane properties (such as membrane material, nature, structure) and operating conditions (such as feed concentration, temperature, driving force, flow rate, etc.) [45]. To some extent, the membrane structure depends on the membrane preparation protocol used [46]. Therefore, since most of the research has been carried out at different operating conditions, it is challenging to provide a fair comparison of PV data among different studies [47]. In this work, we tentatively compare the performance of different membranes (pristine, blend and composites) at close operating conditions, as enlisted in **Table 4.** The main bridle of hydrophilic polymers (like CS) is related to their high swelling tendency which may limit the mechanical properties and stability of the membranes prepared with them. If a membrane is swollen, there is a lack of efficient separation performance due to the polymer chains mobility. Therefore, many efforts have been done to improve the physicochemical properties of CS, by using several approaches such as the blending with polymers, agents and inorganic nanomaterials.

In this work, the best performance, in terms of selectivity, was obtained for the xCS:PRO:SUF membrane, which exhibited a separation factor of 35.4 (at 25 ºC). Such a value corresponds to 3-fold higher separation factor compared with pristine CS membrane; unfortunately, the permeation flux was compromised. When compared with literature, our xCS:PRO:SUF membranes showed better selectivity than other polymers, such as modified polyether ether ketone (PEEKWC), poly(vinyl alcohol) (PVA), acrylic

acid plasma polymerized poly(3-hydroxybutyrate), and composite membranes (GO-polyimide, polyamide filled with Al_2O_3) (see **Table 4**). Definitely, the permeation rate could be improved by handling the operating temperature but it may affect the selective properties.

On the contrary, xCS:PRO:SUF membranes did not show a competitive selectivity in comparison to cellulose acetate/polyvinyl pyrrolidone (PVP), PVA/cellulose acetate blend, cross-linked PVA, cellulose acetate filled with HZSM5 membranes, among other composites. At this point, it is confirmed that these membranes (i.e., xCS:PRO:SUF) are still limited by their selective-permeable trade-off.

Table 4. Comparison of CS-DES membrane performance with some pure polymeric and mixed matrix membranes at close MeOH-MTBE azeotropic conditions.

Membrane material	Filler loading:	MeOH Concentration	Operating conditions	J (kg m^{-2} h^{-1})	Separation factor (α)	Reference:
xCS:PRO:SUF	-	14.3 wt.% MeOH	25 ºC, 0.05 mbar	0.008	35.4	This work
GO-polyimide	4 wt.%	14.3 wt.% MeOH	45 ºC, 0.05 mbar	0.091	9.0	(Castro-Muñoz et al., 2019)
PEEKWC	-	15 wt.% MeOH	40 ºC, 6.1 mbar	0.068	10	[49]
PVA	-	30 wt.% MeOH	45 ºC, 15 mbar	0.900	25	[50]

Polylactic acid	-	15 wt.% MeOH	30 ºC, 6 mbar	0.620	5	[51]
Polylactic acid		14.3 wt.% MeOH	40 ºC, 6.1 mbar	0.090	75	[52]
Cellulose acetate-PVP blend	-	20 wt.% MeOH	45 ºC, 3 mbar	0.225	340	[53]
PVA-cellulose acetate blend	-	15 wt.% MeOH	45 ºC, 17 mbar	796*	1427	[54]
Acrylic acid plasma polymerized poly(3-hydroxybutyrate)	-	20 wt.% MeOH	45 ºC, 1.3 mbar	11*	3	[55]
Cross-linked PVA	-	20 wt.% MeOH	50 ºC, 0.4 mbar	0.036	1230	[56]
Cross-linked PAMHEMA	-	11 wt.% MeOH	50 ºC, 1.33 mbar	0.140	150	[57]
Polyamide filled with Al_2O_3	10 wt.%	50 wt.% MeOH	30 ºC	15*	20	[58]
cellulose acetate filled with HZSM5	0.5 wt.%	20 wt.% MeOH	40 ºC, 3.3 mbar	4.2*	150	[59]
Sulfonated polyarylethersulfone with cardo filled with $[Cu_2(bdc)_2(bpy)]_n$	30 wt.%	15 wt.% MeOH	40 ºC, 6 mbar	0.28	2300	[60]
cellulose acetate filled with ZnO	10 wt.%	31 wt.% MeOH	40 ºC, 5 mbar	2*	400	[61]
Sulfonated polyarylethersulfone with cardo filled with MIL-53(Al)-SO_3H	15 wt.%	15 wt.% MeOH	40 ºC, 6 mbar	0.368	1990	[62]
CS	-	30 wt.% MeOH	50 ºC	0.120	7	[63]

* Normalized flux by thickness.

4. Concluding remarks and future perspectives

In this work, dense CS-hydrophilic L-proline:sulfolane membranes have been, for the first time, successfully prepared and characterized. By fully mapping the structure of the membranes, this study demonstrated complete miscibility and embodiment of the proposed novel hydrophilic DESs (PRO:SUF) into the polymer phase. Importantly, since we have used environmentally friendly materials (such as CS, water, organic DES), these membranes can be considered as pioneering work in manufacturing more sustainable dense bio-based membranes.

After preliminarily testing in MeOH-MTBE separation using PV process, this new concept of membranes (xCS:PRO:SUF) presents a 3-fold higher separation efficiency than the pristine CS. As an outlook, the future works can focus on improving the permeation rates of the membranes in order to make them more attractive for other PV separations. In fact, thanks to their ability in forming H-bonding interactions, DESs may promote an enhanced separation of other polar molecules from azeotropic mixtures [27]. Moreover, the novel membranes, due to their dense nature, can be also interesting to be tested in gas separation applications.

Finally, in view of making the entire fabrication process fully sustainable, GA can be replaced with a more benign cross-linker such as genipin.

Acknowledgments

The authors gratefully acknowledge the financial support from the National Science Centre, Warsaw, Poland – decision no. UMO-2018/30/E/ST8/00642. Financial support from Polish National Agency for Academic Exchange (NAWA) under Ulam Programme

(Agreement No. PPN/ULM/2020/1/00005/U/00001) is gratefully acknowledged. R. Castro-Muñoz also acknowledges the School of Engineering and Science and the FEMSA-Biotechnology Center at Tecnológico de Monterrey for their support through the Bioprocess (0020209I13) Focus Group. The authors also acknowledged Emilia Gontarek for her indispensable support for FTIR and contact angle measurements.

Conflict of Interest

The authors declare no conflict of interest.

References

[1] P.T. Anastas, J.C. Warner, Green Chemistry: Theory and Practice, Green Chem. Theory Pract. Oxford Univ. Press. New York. (1998).

[2] P.T. Anastas, N. Eghbali, Green Chesmitry: Principles and Practice, Chem. Soc. Rev. 39 (2010) 201–312.

[3] E.L. Smith, A.P. Abbott, K.S. Ryder, Deep Eutectic Solvents (DESs) and Their Applications, Chem. Rev. 114 (2014) 11060–11082. https://doi.org/10.1021/cr300162p.

[4] P. Liu, J.W. Hao, L.P. Mo, Z.H. Zhang, Recent advances in the application of deep eutectic solvents as sustainable media as well as catalysts in organic reactions, RSC Adv. 5 (2015) 48675–48704. https://doi.org/10.1039/c5ra05746a.

[5] J. Huang, X. Guo, T. Xu, L. Fan, X. Zhou, S. Wu, Ionic deep eutectic solvents for the extraction and separation of natural products, J. Chromatogr. A. 1598 (2019) 1–19. https://doi.org/10.1016/j.chroma.2019.03.046.

[6] A.R. Harifi-Mood, F. Mohammadpour, G. Boczkaj, Solvent dependency of carbon dioxide Henry's constant in aqueous solutions of choline chloride-ethylene glycol based deep eutectic solvent, J. Mol. Liq. 319 (2020) 114173. https://doi.org/10.1016/j.molliq.2020.114173.

[7] P. Makoś, G. Boczkaj, Deep eutectic solvents based highly efficient extractive desulfurization of fuels – Eco-friendly approach, J. Mol. Liq. 296 (2019) 111916. https://doi.org/10.1016/j.molliq.2019.111916.

[8] M. Momotko, J. Łuczak, A. Przyjazny, G. Boczkaj, First deep eutectic solvent-based (DES) stationary phase for gas chromatography and future perspectives for DES application in separation techniques, J. Chromatogr. A. 1635 (2020) 461701. https://doi.org/10.1016/j.chroma.2020.461701.

[9] F. Merza, A. Fawzy, I. AlNashef, S. Al-Zuhair, H. Taher, Effectiveness of using deep eutectic solvents as an alternative to conventional solvents in enzymatic biodiesel production from waste oils, Energy Reports. 4 (2018) 77–83. https://doi.org/10.1016/j.egyr.2018.01.005.

[10] Y.P. Mbous, M. Hayyan, A. Hayyan, W.F. Wong, M.A. Hashim, C.Y. Looi, Applications of deep eutectic solvents in biotechnology and bioengineering—Promises and challenges, Biotechnol. Adv. 35 (2017) 105–134. https://doi.org/10.1016/j.biotechadv.2016.11.006.

[11] A.E. Ünlü, A. Arlkaya, S. Takaç, Use of deep eutectic solvents as catalyst: A mini-review, Green Process. Synth. 8 (2019) 355–372. https://doi.org/10.1515/gps-2019-0003.

[12] M. Taghizadeh, A. Taghizadeh, V. Vatanpour, M.R. Ganjali, M.R. Saeb, Deep

eutectic solvents in membrane science and technology: Fundamental, preparation, application, and future perspective, Sep. Purif. Technol. 258 (2021) 118015. https://doi.org/10.1016/j.seppur.2020.118015.

[13] B. Jiang, H. Dou, L. Zhang, B. Wang, Y. Sun, H. Yang, Z. Huang, H. Bi, Novel supported liquid membranes based on deep eutectic solvents for olefin-paraffin separation via facilitated transport, J. Memb. Sci. 536 (2017) 123–132. https://doi.org/10.1016/j.memsci.2017.05.004.

[14] Z. Dai, H. Aboukeila, L. Ansaloni, J. Deng, M. Giacinti Baschetti, L. Deng, Nafion/PEG hybrid membrane for CO 2 separation: Effect of PEG on membrane micro-structure and performance, Sep. Purif. Technol. 214 (2019) 67–77. https://doi.org/10.1016/j.seppur.2018.03.062.

[15] Z. Dai, L. Ansaloni, J.J. Ryan, R.J. Spontak, L. Deng, Nafion/IL hybrid membranes with tuned nanostructure for enhanced CO2 separation: Effects of ionic liquid and water vapor, Green Chem. 20 (2018) 1391–1404. https://doi.org/10.1039/c7gc03727a.

[16] N.M. Mahmoodi, M. Taghizadeh, A. Taghizadeh, Activated carbon/metal-organic framework composite as a bio-based novel green adsorbent: Preparation and mathematical pollutant removal modeling, J. Mol. Liq. 277 (2019) 310–322. https://doi.org/10.1016/j.molliq.2018.12.050.

[17] B. Jiang, N. Zhang, L. Zhang, Y. Sun, Z. Huang, B. Wang, H. Dou, H. Guan, Enhanced separation performance of PES ultrafiltration membranes by imidazole-based deep eutectic solvents as novel functional additives, J. Memb. Sci. 564 (2018) 247–258. https://doi.org/10.1016/j.memsci.2018.07.034.

[18] P.G. Ingole, N.R. Thakare, K. Kim, H.C. Bajaj, K. Singh, H. Lee, Preparation, characterization and performance evaluation of separation of alcohol using crosslinked membrane materials, New J. Chem. 37 (2013) 4018–4024. https://doi.org/10.1039/c3nj00952a.

[19] N. Ptaszyńska, K. Gucwa, K. Olkiewicz, M. Heldt, M. Serocki, A. Stupak, D. Martynow, D. Dębowski, A. Gitlin-Domagalska, J. Lica, A. Łęgowska, S. Milewski, K. Rolka, Conjugates of ciprofloxacin and levofloxacin with cell-penetrating peptide exhibit antifungal activity and mammalian cytotoxicity, Int. J. Mol. Sci. 21 (2020) 1–25. https://doi.org/10.3390/ijms21134696.

[20] R. Castro-Muñoz, F. Galiano, V. Fíla, E. Drioli, A. Figoli, Matrimid ® 5218 dense membrane for the separation of azeotropic MeOH- MTBE mixtures by pervaporation, Sep. Purif. Technol. 199 (2018) 27–36. https://doi.org/10.1016/j.seppur.2018.01.045.

[21] E.P. Favvas, A. Figoli, R. Castro-Muñoz, V. Fíla, X. He, Polymeric membrane materials for CO2 separations, 2018. https://doi.org/10.1016/B978-0-12-813645-4.00001-5.

[22] H.G. Premakshi, K. Ramesh, M.Y. Kariduraganavar, Modification of crosslinked chitosan membrane using NaY zeolite for pervaporation separation of water-isopropanol mixtures, Chem. Eng. Res. Des. 94 (2015) 32–43. https://doi.org/10.1016/j.cherd.2014.11.014.

[23] M. Loloei, M. Omidkhah, A. Moghadassi, A.E. Amooghin, Preparation and characterization of Matrimid® 5218 based binary and ternary mixed matrix membranes for CO2 separation, Int. J. Greenh. Gas Control. 39 (2015) 225–235.

https://doi.org/http://dx.doi.org/10.1016/j.ijggc.2015.04.016.

[24] R. Castro-Muñoz, V. Fíla, M.Z. Ahmad, Enhancing the CO 2 Separation Performance of Matrimid 5218 Membranes for CO 2 /CH 4 Binary Mixtures, Chem. Eng. Technol. (2019) ceat.201800111. https://doi.org/10.1002/ceat.201800111.

[25] B. Jiang, N. Zhang, B. Wang, N. Yang, Z. Huang, H. Yang, Z. Shu, Deep eutectic solvent as novel additive for PES membrane with improved performance, Sep. Purif. Technol. 194 (2018) 239–248. https://doi.org/10.1016/j.seppur.2017.11.036.

[26] F. Russo, R. Castro-Muñoz, F. Galiano, A. Figoli, Unprecedented preparation of porous Matrimid ® 5218 membranes, J. Memb. Sci. (2019). https://doi.org/10.1016/j.memsci.2019.05.036.

[27] M.K. Hadj-Kali, H.F. Hizaddin, I. Wazeer, L. El blidi, S. Mulyono, M.A. Hashim, Liquid-liquid separation of azeotropic mixtures of ethanol/alkanes using deep eutectic solvents: COSMO-RS prediction and experimental validation, Fluid Phase Equilib. 448 (2017) 105–115. https://doi.org/10.1016/j.fluid.2017.05.021.

[28] A. Pandey, R. Rai, M. Pal, S. Pandey, How polar are choline chloride-based deep eutectic solvents?, Phys. Chem. Chem. Phys. 16 (2014) 1559–1568. https://doi.org/10.1039/c3cp53456a.

[29] I.M. Arcana, B. Bundjali, I. Yudistira, B. Jariah, L. Sukria, Study on properties of polymer blends from polypropylene with polycaprolactone and their biodegradability, Polym. J. 39 (2007) 1337–1344. https://doi.org/10.1295/polymj.PJ2006250.

[30] R. Castro-Muñoz, M.Z. Ahmad, V. Fíla, Tuning of Nano-Based Materials for

Embedding Into Low-Permeability Polyimides for a Featured Gas Separation, Front. Chem. 7 (2020) 1–14. https://doi.org/10.3389/fchem.2019.00897.

[31] R. Castro-Muñoz, J. González-Valdez, M.Z. Ahmad, High-performance pervaporation chitosan-based membranes: new insights and perspectives, Rev. Chem. Eng. (2020) 20190051. https://doi.org/https://doi.org/10.1515/revce-2019-0051.

[32] H.S. Tsai, Y.Z. Wang, Properties of hydrophilic chitosan network membranes by introducing binary crosslink agents, Polym. Bull. 60 (2008) 103–113. https://doi.org/10.1007/s00289-007-0846-x.

[33] J.Z. Knaul, S.M. Hudson, K.A.M. Creber, Crosslinking of chitosan fibers with dialdehydes: Proposal of a new reaction mechanism, J. Polym. Sci. Part B Polym. Phys. 37 (1999) 1079–1094. https://doi.org/10.1002/(SICI)1099-0488(19990601)37:11<1079::AID-POLB4>3.0.CO;2-O.

[34] R.S. Vieira, M.M. Beppu, Interaction of natural and crosslinked chitosan membranes with Hg(II) ions, Colloids Surfaces A Physicochem. Eng. Asp. 279 (2006) 196–207. https://doi.org/10.1016/j.colsurfa.2006.01.026.

[35] S.P. Dharupaneedi, R. V. Anjanapura, J.M. Han, T.M. Aminabhavi, Functionalized graphene sheets embedded in chitosan nanocomposite membranes for ethanol and isopropanol dehydration via pervaporation, Ind. Eng. Chem. Res. 53 (2014) 14474–14484. https://doi.org/10.1021/ie502751h.

[36] M. Kong, X.G. Chen, K. Xing, H.J. Park, Antimicrobial properties of chitosan and mode of action: A state of the art review, Int. J. Food Microbiol. 144 (2010) 51–63. https://doi.org/10.1016/j.ijfoodmicro.2010.09.012.

[37] M. Mathaba, M.O. Daramola, Effect of chitosan's degree of deacetylation on the performance of pes membrane infused with chitosan during amd treatment, Membranes (Basel). 10 (2020). https://doi.org/10.3390/membranes10030052.

[38] T.Y. Hsien, G.L. Rorrer, Effects of Acylation and Crosslinking on the Material Properties and Cadmium Ion Adsorption Capacity of Porous Chitosan Beads, Sep. Sci. Technol. 30 (1995) 2455–2475. https://doi.org/10.1080/01496399508021395.

[39] J.R. Rodríguez-Núñez, T.J. Madera-Santana, D.I. Sánchez-Machado, J. López-Cervantes, H. Soto Valdez, Chitosan/Hydrophilic Plasticizer-Based Films: Preparation, Physicochemical and Antimicrobial Properties, J. Polym. Environ. 22 (2014) 41–51. https://doi.org/10.1007/s10924-013-0621-z.

[40] Y. Pranoto, S.K. Rakshit, V.M. Salokhe, Enhancing antimicrobial activity of chitosan films by incorporating garlic oil, potassium sorbate and nisin, LWT - Food Sci. Technol. 38 (2005) 859–865. https://doi.org/10.1016/j.lwt.2004.09.014.

[41] E. Jakubowska, M. Gierszewska, J. Nowaczyk, E. Olewnik-Kruszkowska, Physicochemical and storage properties of chitosan-based films plasticized with deep eutectic solvent, Food Hydrocoll. 108 (2020) 106007. https://doi.org/10.1016/j.foodhyd.2020.106007.

[42] C. Nagel, K. Günther-Schade, D. Fritsch, T. Strunskus, F. Faupel, Free volume and transport properties in highly selective polymer membranes, Macromolecules. 35 (2002) 2071–2077. https://doi.org/10.1021/ma011028d.

[43] R. Huang, C. Yeom, Pervaporation separation of aqueous mixtures using crosslinked poly(vinyl alcohol)(pva). II. Permeation of ethanol-water mixtures, J.

Memb. Sci. 51 (1990) 273–292.

[44] Y.L. Xue, J. Huang, C.H. Lau, B. Cao, P. Li, Tailoring the molecular structure of crosslinked polymers for pervaporation desalination, Nat. Commun. 11 (2020) 1461. https://doi.org/10.1038/s41467-020-15038-w.

[45] F. Galiano, F. Falbo, A. Figoli, Polymeric Pervaporation Membranes: Organic-Organic Separation, 2016. https://doi.org/10.1002/9781118831823.ch7.

[46] M. Rezakazemi, A. Ebadi Amooghin, M.M. Montazer-Rahmati, A.F. Ismail, T. Matsuura, State-of-the-art membrane based CO2 separation using mixed matrix membranes (MMMs): An overview on current status and future directions, Prog. Polym. Sci. (2014). https://doi.org/10.1016/j.progpolymsci.2014.01.003.

[47] A. Figoli, S. Santoro, F. Galiano, A. Basile, Pervaporation membranes: preparation, characterization, and application, in: A. Basile, A. Figoli, M. Khayet (Eds.), Pervaporation, Vap. Permeat. Membr. Distill., First edit, Elsevier Ltd., Cambridge UK, 2015: pp. 281–304.

[48] R. Castro-Muñoz, F. Galiano, Ó. de la Iglesia, V. Fíla, C. Téllez, J. Coronas, A. Figoli, Graphene oxide – Filled polyimide membranes in pervaporative separation of azeotropic methanol–MTBE mixtures, Sep. Purif. Technol. 224 (2019) 265–272. https://doi.org/10.1016/j.seppur.2019.05.034.

[49] S. Zereshki, A. Figoli, S.S. Madaeni, S. Simone, M. Esmailinezhad, E. Drioli, Pervaporation separation of MeOH/MTBE mixtures with modified PEEK membrane: Effect of operating conditions, J. Memb. Sci. 371 (2011) 1–9. https://doi.org/10.1016/j.memsci.2010.11.068.

[50] M. Peivasti, A. Madandar, T. Mohammadi, Effect of operating conditions on

pervaporation of methanol / methyl tert -butyl ether mixtures, 47 (2008) 1069–1074. https://doi.org/10.1016/j.cep.2007.08.005.

[51] S. Zereshki, A. Figoli, S.S. Madaeni, S. Simone, E. Drioli, Pervaporation Separation of Methanol / Methyl tert -Butyl Ether with Poly (lactic acid) Membranes, J. Appl. Polym. Sci. 118 (2010) 1364–1371. https://doi.org/10.1002/app.

[52] F. Galiano, A.H. Ghanim, K.T. Rashid, T. Marino, S. Simone, Q.F. Alsalhy, A. Figoli, Preparation and characterization of green polylactic acid (PLA) membranes for organic/organic separation by pervaporation, Clean Technol. Environ. Policy. 21 (2019) 109–120. https://doi.org/10.1007/s10098-018-1621-4.

[53] H. Wu, X. Fang, X. Zhang, Z. Jiang, B. Li, X. Ma, Cellulose acetate – poly (N-vinyl-2-pyrrolidone) blend membrane for pervaporation separation of methanol / MTBE mixtures, 64 (2008) 183–191. https://doi.org/10.1016/j.seppur.2008.09.013.

[54] K. Zhou, Q. Gen, G.L. Han, A.M. Zhu, Q. Lin, Pervaporation of water – ethanol and methanol – MTBE mixtures using poly (vinyl alcohol)/ cellulose acetate blended membranes, J. Memb. Sci. 448 (2013) 93–101. https://doi.org/10.1016/j.memsci.2013.08.005.

[55] M. Villegas, A.I. Romero, M.L. Parentis, E.F.C. Vidaurre, J.C. Gottifredi, Chemical Engineering Research and Design Acrylic acid plasma polymerized poly (3-hydroxybutyrate) membranes for methanol / MTBE separation by pervaporation, Chem. Eng. Res. Des. 109 (2016) 234–248. https://doi.org/10.1016/j.cherd.2016.01.018.

[56] J. Rhim, Y. Kim, Pervaporation Separation of MTBE – Methanol Mixtures Using

Cross-linked PVA Membranes, (1999) 1699–1707.

[57] S. Ray, S.K. Ray, Synthesis of highly methanol selective membranes for separation of methyl tertiary butyl ether (MTBE)– methanol mixtures by pervaporation, 278 (2006) 279–289. https://doi.org/10.1016/j.memsci.2005.11.011.

[58] R. Kopec, M. Meller, W. Kujawski, J. Kujawa, Polyamide-6 based pervaporation membranes for organic-organic separation, Sep. Purif. Technol. 110 (2013) 63–73. https://doi.org/10.1016/j.seppur.2013.03.007.

[59] X. Ma, C. Hu, R. Guo, X. Fang, H. Wu, Z. Jiang, HZSM5-filled cellulose acetate membranes for pervaporation separation of methanol/MTBE mixtures, Sep. Purif. Technol. 59 (2008) 34–42. https://doi.org/10.1016/j.seppur.2007.05.023.

[60] G.L. Han, K. Zhou, A.N. Lai, Q.G. Zhang, A.M. Zhu, Q. Lin, [Cu 2 (bdc) 2 (bpy)] n / SPES-C mixed matrix membranes for separation of methanol / methyl tert-butyl ether mixtures, J. Memb. Sci. 454 (2014) 36–43. https://doi.org/10.1016/j.memsci.2013.11.049.

[61] Y. Wang, L. Yang, G. Luo, Y. Dai, Preparation of cellulose acetate membrane filled with metal oxide particles for the pervaporation separation of methanol/methyl tert-butyl ether mixtures, Chem. Eng. J. 146 (2009) 6–10. https://doi.org/10.1016/j.cej.2008.05.009.

[62] G.L. Han, Z. Chen, L.F. Cai, Y.H. Zhang, J.F. Tian, H.H. Ma, S.M. Fang, Post-synthetic MIL-53(Al)-SO3 H incorporated sulfonated polyarylethersulfone with cardo (SPES-C) membranes for separating methanol and methyl tert-butyl ether mixture, Sep. Purif. Technol. 220 (2019) 268–275.

https://doi.org/10.1016/j.seppur.2019.03.065.

[63] M.G. Mohd Nawawi, Z. Zamrud, Z. Idham, O. Hassan, N.M. Sakri, Blended Chitosan and Polyvinyl Alcohol Membrane for Pervaporation Operating Parameters, J. Teknol. (Sciences Eng. 65 (2013) 39–43.